Published in final edited form as:
Circ Res. 2015 February 27; 116(5): 846–856. doi:10.1161/CIRCRESAHA.116.305404.

The Mechanisms of Calcium Cycling and Action Potential Dynamics in Cardiac Alternans

Giedrius Kanaporis and **Lothar A. Blatter**
Department of Molecular Biophysics and Physiology, Rush University Medical Center, Chicago, IL 60612, USA

Abstract

Rationale—Alternans is a risk factor for cardiac arrhythmia, including atrial fibrillation. At the cellular level alternans manifests as beat-to-beat alternations in contraction, action potential duration (APD) and magnitude of the Ca^{2+} transient (CaT). Electromechanical and CaT alternans are highly correlated, however it has remained controversial whether the primary cause of alternans is a disturbance of cellular Ca^{2+} signaling or electrical membrane properties.

Objective—Determine whether a primary failure of intracellular Ca^{2+} regulation or disturbances in V_m and AP regulation are responsible for the occurrence of alternans in atrial myocytes.

Methods and Results—Pacing-induced APD and CaT alternans were studied in single rabbit atrial and ventricular myocytes using combined $[Ca^{2+}]_i$ and electrophysiological measurements. In current-clamp experiments APD and CaT alternans strongly correlated in time and magnitude. CaT alternans was observed without alternation in L-type Ca^{2+} current, however, elimination of intracellular Ca^{2+} release abolished APD alternans, indicating that $[Ca^{2+}]_i$ dynamics have a profound effect on the occurrence of CaT alternans. Trains of two distinctive voltage commands in form of APs recorded during large and small alternans CaTs, were applied to voltage-clamped cells. CaT alternans were observed with and without alternation in the voltage command shape. During ‘alternans AP-clamp’ large CaTs coincided with both long and short AP waveforms, indicating that CaT alternans develop irrespective of AP dynamics.

Conclusion—The primary mechanism underlying alternans in atrial cells, similarly to ventricular cells, resides in a disturbance of Ca^{2+} signaling while APD alternans are a secondary consequence, mediated by Ca^{2+}-dependent AP modulation.

Keywords

Alternans; action potential; Ca signaling; excitation-contraction coupling; arrhythmia

Address correspondence to: Dr. Lothar A. Blatter, Department of Molecular Biophysics and Physiology, Rush University Medical Center, 1750 W. Harrison Street, Chicago, IL 60612, USA, Tel: 312-563-3238, Fax: 312-942-8711, Lothar_Blatter@rush.edu.

DISCLOSURES
None.

INTRODUCTION

Cardiac alternans is a recognized risk factor for cardiac arrhythmia, including atrial fibrillation[1–3], and sudden cardiac death[4, 5]. T-wave alternans in the electrocardiogram, corresponding to beat-to-beat alternations in ventricular repolarization, has become a prognostic tool for arrhythmia risk stratification and guidance of antiarrhythmic therapy[6, 7]. At the cellular level cardiac alternans is defined as cyclic, beat-to-beat variations in contraction amplitude (mechanical alternans), action potential duration (APD or electrical alternans) and cytosolic Ca^{2+} transient (CaT) amplitude at constant stimulation frequency (e.g.[8]). A plethora of experimental conditions and interventions have been demonstrated to cause and modulate cardiac alternans, suggesting a multifactorial process (for reviews see[9–14]). In cardiac myocytes the beat-to-beat regulation of cytosolic calcium ($[Ca^{2+}]_i$) and membrane potential (V_m) is bi-directionally coupled and involves complex feedback mechanisms, often mediated by Ca^{2+}-dependent membrane conductances, that link these two parameters. It is generally agreed that this relationship represents a key causative factor for electromechanical and CaT alternans (summarized e.g. in [9]). The question whether $V_m \rightarrow [Ca^{2+}]_i$ or $[Ca^{2+}]_i \rightarrow V_m$ coupling is the primary underlying mechanism for alternans has been addressed almost exclusively in ventricular myocytes, but not in atria. It was suggested that at high stimulation rates V_m alternations are determined by APD restitution and is an underlying cause for the development of alternans ($V_m \rightarrow [Ca^{2+}]_i$)[15]. APD restitution refers to the APD dependence on the preceding diastolic interval and, if this relationship is steep enough, self-sustaining oscillations of APD can occur[16–20]. In this case the time-dependent recovery of ion channels from inactivation, in particular recovery of L-type Ca^{2+} channels (LCC), has been hypothesized as a causative factor for the generation of alternans[17, 21, 22]. Conversely, other studies demonstrated a poor relationship between experimentally determined APD restitution kinetics and occurrence of alternans[23–26], and it was suggested that disturbances in beat-to-beat Ca^{2+} cycling constitute the main cause of cardiac alternans ($[Ca^{2+}]_i \rightarrow V_m$)[22, 27–30]. In this case V_m is determined by the effect and consequences of $[Ca^{2+}]_i$ dynamics, Ca^{2+} fluxes and Ca^{2+}-dependent ion currents and transporters.

In light of these unresolved issues we set out to determine the detailed effects of AP morphology on the occurrence of CaT alternans in atrial myocytes where V_m $[Ca^{2+}]_i$ coupling has not been investigated systematically despite the fact that atrial fibrillation is the most common cardiac arrhythmia[31] and has been causally linked to alternans[1–3, 32]. While it is anticipated that mechanisms of alternans in atrial and ventricular cells share similarities, significant differences are also expected. Atrial and ventricular cells exhibit distinctive differences in Ca^{2+} cycling during excitation-contraction coupling (ECC) due to the lack of or poor development and irregular organization of transverse (t)-tubules[33–35] and higher sarcoplasmic/endoplasmic reticulum Ca^{2+} ATPase (SERCA) activity[36–38] in the atria. Computer simulations using cell models with and without t-tubules have predicted significant differences in possible alternans mechanisms[39–41]. This has potentially important ramifications for the understanding of Ca^{2+} cycling, ECC and arrhythmic disturbances in cardiac disease. Ventricular myocytes from diseased heart (myocardial infarction, heart failure, atrial fibrillation) often undergo a dramatic loss and disruption of the t-tubule system[42–45] and become functionally and structurally reminiscent of atrial cells. In addition

to the differences in t-tubule system, atrial and ventricular cells also contain unique sets of ion channels[46, 47] leading to distinctive AP morphology and Ca^{2+}-dependent modulation of APD. To investigate the role of V_m $[Ca^{2+}]_i$ coupling, we have combined $[Ca^{2+}]_i$ measurements with the voltage clamp technique and subjected cardiac myocytes to a number of different voltage clamp protocols, including AP-clamp protocols in form of constant shape APs or APD alternans. To compare alternans mechanisms in atrial and ventricular cells analogous experiments using the same experimental conditions were performed on ventricular myocytes as well. In summary, the data reveal that 1) CaT alternans in atrial myocytes can develop in the absence of APD alternans; 2) alternans AP clamp protocol do not lead obligatorily to CaT alternans; 3) when alternans AP voltage clamp induced CaT alternans, large amplitude CaTs were observed coinciding with AP waveforms that were recorded previously during both, a small amplitude as well as a large amplitude of alternating CaTs; 4) suppression of Ca^{2+} release from sarcoplasmic reticulum (SR) abolishes APD alternans; and 5) atrial cells exhibit more pronounced APD alternans than ventricular cells. These data show that atrial and ventricular myocytes share similarities with respect to alternans mechanisms but also exhibit important differences, and the role of $V_m \rightarrow [Ca^{2+}]_i$ coupling for the generation of electromechanical alternans is likely secondary to the disturbances in Ca^{2+} signaling.

METHODS

Detailed methods are provided in the Online Supplement.

Cell isolation

Ventricular and atrial myocytes were enzymatically isolated from New Zealand White rabbits via Langendorff perfusion. All procedures and protocols involving animals conform to the Guide for the Care and Use of Laboratory Animals of the National Institutes of Health, and were approved by the Institutional Animal Care and Use Committee.

Electrophysiological measurements

Electrophysiological recordings were made in the ruptured whole-cell patch clamp configuration using an Axopatch 200A patch-clamp amplifier. For AP measurements the whole-cell current clamp mode was used. For I_{LCC} measurements membrane currents were elicited by 100 ms depolarization steps to 0 mV from a holding potential of -50 mV. For AP-clamp experiments voltage commands were derived from previously recorded atrial or ventricular AP-waveforms.

Cytosolic $[Ca^{2+}]_i$ measurements

Simultaneously with electrophysiological recordings cytosolic $[Ca^{2+}]_i$ was recorded using Fluo-4 or Indo-1 pentapotassium salts added to the patch pipette solution. Fluo-4 was excited with a 488-nm argon ion laser and recorded at 515 nm. Fluo-4 emission signals (F) were background subtracted and normalized to baseline fluorescence (F_0), and changes of $[Ca^{2+}]_i$ are presented as F/F_0. Indo-1 was excited at 357 nm and emission was recorded simultaneously at 410 nm (F_{410}) and 485 nm (F_{485}) via photomultiplier tubes. F_{410} and F_{485} signals were background subtracted and changes of $[Ca^{2+}]_i$ are expressed as changes of

$R=F_{410}/F_{485}$. CaT alternans was induced by increasing the pacing frequency until stable CaT alternans was observed. The degree of CaT alternans was quantified as the alternans ratio (AR), defined as $AR=1-CaT_{Small}/CaT_{Large}$, where CaT_{Small} and CaT_{Large} are the small- and large-amplitude CaTs from a pair of alternating CaTs. All experiments were carried out at room temperature (20–22°C).

Data analysis and presentation

Results are presented as individual observations or as means ± SEM of n cells. Statistical significance was evaluated using Student's t-test and differences were considered significant at $p<0.05$.

RESULTS

Beat-to-beat AP morphology during CaT alternans

Alternans was induced by incrementally increasing the rate of electrical pacing of current-clamped myocytes. Increasing the pacing rate eventually led to the simultaneous onset of beat-to-beat alternations in both CaT amplitude and AP morphology (the threshold frequencies where alternans was induced are summarized in Supplemental Figure I). Fig. 1 shows examples of simultaneous recordings of APs and CaTs from single atrial (Fig. 1A) and ventricular (Fig. 1C) cells. In all cells tested the onset of APD alternans coincided in time with the onset of CaT alternans. Figs. 1B and 1D show superimposed APs recorded simultaneously with large (AP_{CaT_Large}) and small (AP_{CaT_Small}) amplitude CaTs from atrial and ventricular cells. The AP waveforms shown here reflect an average of three consecutive AP recordings. In both atrial and ventricular cells, AP_{CaT_Small} exhibited a more pronounced plateau phase followed by steeper repolarization compared to AP_{CaT_Large}. APD at 30, 50 and 90% repolarization (APD30, APD50 and APD90) for AP_{CaT_Large} and AP_{CaT_Small} were compared. AP_{CaT_Small} increased in duration at APD30 and shortened at APD90 level. While changes in APD50 were small, the majority of atrial and ventricular cells exhibited a slightly wider APD50 during the small amplitude CaT. In atrial myocytes exhibiting an average CaT alternans ratio (AR) of 0.64 ± 0.04, $APD30_{CaT\_Small}$ and $APD50_{CaT\_Small}$ increased by 86 ± 11 and 26 ± 8%, respectively, while $APD90_{CaT\_Small}$ decreased by 12 ± 5% (n=14). In ventricular myocytes CaTs alternated with an average AR of 0.55 ± 0.09. $APD30_{CaT\_Small}$ and $APD50_{CaT\_Small}$ increased by 32 ± 6% and 3 ± 3%, respectively, and $APD90_{CaT\_Small}$ shortened by 8 ± 3% (n=10).

In both atrial and ventricular myocytes, changes in APD correlated with the CaT AR, indicating a tight link between APD and CaT alternans. For each cell tested, $APD_{CaT\_Small}/APD_{CaT\_Large}$ ratios were plotted *versus* AR of the CaTs and fitted with a linear regression function to help categorize the data. Fig. 2 shows that for APD30 and APD50, $APD_{CaT\_Small}/APD_{CaT\_Large}$ ratios increased with increasing AR, whereas for APD90 the $APD_{CaT\_Small}/APD_{CaT\_Large}$ ratio slightly decreased in both atrial (Fig. 2A) and ventricular (Fig. 2C) cells (data derived from the same cells as shown in Fig. 1). Linear regression slopes for all individual cells, as well as the averages for each data set are presented in Figs. 2B and 2D.

In conclusion, the onset and progression of APD alternans in cardiac myocytes correlated with the alternation in $[Ca^{2+}]_i$ in time and magnitude. AP_{CaT_Small} recorded during a small amplitude alternans CaT exhibited a more prominent plateau phase and showed faster repolarization resulting in an increase of APD30 and APD50, and a shortening of APD90. The most pronounced beat-to-beat alternation was observed at APD30 level in both atrial and ventricular cells. Thus, while qualitative changes in APDs at different degrees of repolarization were the same in atrial and ventricular cell, overall the beat-to-beat differences in APD were clearly more pronounced in atrial myocytes.

Ca^{2+} transients are not driven by the changes in AP morphology

To gain further insight whether cardiac alternans is driven by disturbances of electrical membrane properties and alternating changes in inherent AP characteristics ($V_m \rightarrow [Ca^{2+}]_i$ coupling) or is caused by a primary defect in intracellular Ca^{2+} cycling ($[Ca^{2+}]_i \rightarrow V_m$ coupling), we conducted several series of AP-clamp experiments combined with simultaneous measurements of $[Ca^{2+}]_i$. For this purpose atrial and ventricular myocytes were voltage-clamped with a voltage command in form of APs that were previously recorded in current clamp mode from the respective cell type exhibiting CaT alternans. AP-clamp voltage protocols were then constructed as a series of AP-waveforms consisting: 1) exclusively of APs recorded during a large amplitude alternans CaT (AP_{CaT_Large}-AP_{CaT_Large} protocol); 2) exclusively of AP_{CaT_Small} recorded during a small amplitude alternans CaT (AP_{CaT_Small}-AP_{CaT_Small} protocol); and 3) of alternating APD (AP_{CaT_Large}-AP_{CaT_Small} protocol, also referred to here as ‘alternans AP clamp’). Atrial and ventricular AP_{CaT_Small} and AP_{CaT_Large} morphologies were discussed in Fig. 1.

In the first set of experiments, cells were paced by a series of AP-waveform commands of the same shape (AP_{CaT_Large}-AP_{CaT_Large} and AP_{CaT_Small}-AP_{CaT_Small} pacing protocols) and under these conditions membrane voltage was identical from beat-to-beat. Both AP_{CaT_Large}-AP_{CaT_Large} and AP_{CaT_Small}-AP_{CaT_Small} pacing protocols induced CaT alternans in atrial (n=9; Fig. 3A,B) and ventricular myocytes (n=10; Fig. 3C,D). The pacing rates required to induce CaT alternans with these protocols varied from 1 to 1.6 Hz (see also Suppl. Fig. I for average alternans induction thresholds) and thus, were in a similar range as in current clamp experiments (Fig. 1). These data indicate that beat-to-beat alternation in the intracellular Ca^{2+} release does not require APD alternans and are consistent with previous findings in isolated ventricular myocytes[29, 30]. Here it is demonstrated that atrial cells exhibit similar behavior and CaT alternans can develop independently of membrane voltage and in the absence of APD alternans.

In the next set of experiment a true ‘alternans AP clamp’ (AP_{CaT_Large}-AP_{CaT_Small}) protocol was applied. When pacing frequency was reduced below alternans inducing threshold CaT alternans disappeared despite the alternating AP voltage commands (Fig. 4 A,B) in both atrial and ventricular myocytes. At higher pacing frequencies (ranging from 1 to 1.8 Hz in atrial and from 0.8 to 1.6 Hz in ventricular myocytes; see also Suppl. Fig. I) CaT alternans could be elicited reliably (Fig. 4 C,D). We analyzed how the amplitude of the CaTs correlated with AP_{CaT_Large} or AP_{CaT_Small} voltage pacing commands during the alternans AP clamp protocol. For this discussion we refer to the situation where the

AP_{CaT_Large} elicited a large amplitude CaT and the AP_{CaT_Small} triggered a small amplitude CaT as “in-phase”, whereas the coincidence of AP_{CaT_Small} and large amplitude CaT (and vice versa) is termed “out-of-phase”. While “out-of-phase” alternans was observed in both atrial and ventricular myocytes, atrial cells revealed a higher propensity of “in-phase” alternans compared to ventricular cells (Fig. 4E). In ventricular myocytes out of 15 cells tested, in 4 cells CaT alternans was exclusively “in-phase”, 9 cells exhibited both “in-phase” and “out-of-phase” alternans, and in two cells only “out-of-phase” alternans was observed, thus no clear tendency in favor of “in-phase” *versus* “out-of-phase” alternans could be identified. In contrast, in 8 atrial cells only “in-phase” CaT alternans was observed and 6 cells exhibited both “in-phase” and “out-of-phase” alternans, whereas no atrial cells that would develop exclusively “out-of-phase” alternans were observed (total n=14 cells).

In summary, our data show that under voltage-clamp conditions CaT alternans develop in the absence or presence of APD (or electrical) alternans. Furthermore, CaT alternans can develop irrespective of AP dynamics and can be “in-phase” or “out-of-phase” as defined above. In addition, CaT alternans can even be absent despite APD alternans. These data are strong indication that CaT alternans results from intrinsic properties of intracellular Ca^{2+} handling, and changes in APD alone are not sufficient to cause CaT alternans. Thus, the results strongly support a $[Ca^{2+}]_i \rightarrow V_m$ coupling paradigm for the genesis of electromechanical alternans. Furthermore, at first approximation atrial and ventricular cells behaved similarly during alternans AP clamp experiments: both cell types revealed “in-phase” and “out-of-phase” alternans, however there were subtle differences in the relative frequency and prevalence of the two forms of alternans.

Changes in L-type Ca^{2+} current are not required for CaT alternans

It has been suggested that APD alternans and alternations in AP morphology might reflect beat-to-beat changes in I_{LCC} [48–50]. Since we observed the largest beat-to-beat APD variability at APD30, i.e. at a voltage near the plateau phase of the AP (Fig. 1) where I_{LCC} contributes to AP morphology, the hypothesis was tested whether beat–to-beat changes in I_{LCC} are required for the induction of CaT alternans. For reasons of comparison between atrial and ventricular cells identical experiments were performed in both cell types. Figure 5A shows simultaneous recordings of I_{LCC} and CaTs in a voltage-clamped ventricular myocyte. I_{LCC} was activated by a 100 ms voltage step from a holding potential of -50 mV to 0 mV. Peak I_{LCC} was measured as the difference between the peak of the inward current and the current level at the end of 100 ms pulse. The stimulation rate varied from 1.3 Hz to 2 Hz to initiate CaT alternans and the average threshold frequency was slightly higher than in current- and AP-clamp experiments (Suppl. Fig. I). In the example shown (Fig. 5A), CaT alternans with an AR of 0.29 was observed at the stimulation rate of 1.3 Hz. In both cell types CaT alternans were induced by the conventional square pulse voltage protocols and were observed without apparent alternation in peak I_{LCC}. The average ratios of peak I_{LCC} (Fig. 5B) measured during a small ($I_{LCC,S}$) and a large ($I_{LCC,L}$) amplitude CaT were 0.99 ± 0.01 and 0.97 ± 0.05 in atrial (n=4) and ventricular (n=5) cells, respectively. In contrast, the simultaneously recorded CaT ARs were 0.35 ± 0.06 and 0.42 ± 0.12. I_{LCC} recorded simultaneously with the small-amplitude CaT exhibited slightly slower inactivation, presumably due to reduced Ca^{2+}-dependent inactivation (CDI).

In summary, with respect to the relationship between I_{LCC} and CaT alternans, these experiments indicate that 1) CaT alternans can be induced without significant beat-to-beat variations in peak I_{LCC}; 2) CaT alternans can be elicited with a conventional square pulse voltage protocols, an observation that provides additional support for the concept that $V_m \rightarrow [Ca^{2+}]_i$ coupling is not a causative factor for cardiac alternans; and 3) since CDI of I_{LCC} is reduced during the small amplitude CaT, I_{LCC} is likely to contribute to the prolongation of APD30 observed during the small amplitude CaT (Fig. 1), indicating the importance of feedback mechanisms for the regulation of V_m $[Ca^{2+}]_i$ coupling.

Inhibition of SR Ca^{2+} release abolishes APD alternans

To further test the hypothesis that APD alternans is driven by alternations in $[Ca^{2+}]_i$, intracellular Ca^{2+} release was inhibited by application of 10 μmol/L ryanodine. Fig. 6A shows APs and simultaneously recorded CaTs before and after application of ryanodine. The average CaT AR before application of ryanodine was 0.72 ± 0.06 (n=4). The data summarized in Fig. 6B show that the application of ryanodine eliminated APD alternans and significantly reduced $APD30_{CaT\_Small}/APD30_{CaT\_Large}$ ratios from 1.98 ± 0.30 observed in control to 1.11 ± 0.04 ($p<0.01$) and $APD50_{CaT\_Small}/APD50_{CaT\_Large}$ from 1.25 ± 0.12 to 1.08 ± 0.03 ($p<0.05$). $APD90_{CaT\_Small}/APD90_{CaT\_Large}$ ratios were 1.03 ± 0.07 and 1.03 ± 0.04 before and after application of ryanodine, respectively (absolute APD30, APD50 and APD90 data are presented in Supplemental Fig. II). Similar results were observed in ventricular cells (data not shown) and are in line with previous observations that inhibition of SR release abolishes APD alternans in ventricle of the whole heart[51, 52] and in single ventricular myocytes[22].

In summary, the results demonstrate that suppression of SR Ca^{2+} release abolished beat-to beat alternation in APD, further supporting the notion that instabilities in intracellular Ca^{2+} handling represent a key factor in the development of APD alternans.

DISCUSSION

In this study, we investigated the interplay between electrical membrane properties and the beat-to-beat $[Ca^{2+}]_i$ dynamics that result in the occurrence of cardiac alternans in atrial and ventricular myocytes. The key findings are: 1) Current clamp experiments revealed that APD and CaT alternans strongly correlated in time and magnitude in both atrial and ventricular cells, but the beat-to-beat difference in APD was significantly larger in atrial cells; 2) CaT alternans was observed without changes in peak I_{LCC}, however during the large amplitude CaT CDI of I_{LCC} was more pronounced; 3) voltage-clamp experiments using AP clamp protocols revealed that CaT alternans occurred irrespective of whether cells were stimulated with a series of same-shape AP-clamp protocols or with alternans AP clamp protocols. During the alternans AP clamp protocol no alternans, “in-phase” and “out-of-phase” (as specifically defined above) CaT alternans was observed, indicating that CaT alternans can develop irrespective of AP dynamics; 4) Elimination of SR Ca^{2+} release abolished APD alternans in atrial myocytes, demonstrating that beat-to-beat $[Ca^{2+}]_i$ dynamics have a profound effect on the occurrence of electrical alternans, thus emphasizing the importance of $[Ca^{2+}]_i \rightarrow V_m$ coupling for the mechanism of alternans.

Role of bi-directional coupling of $[Ca^{2+}]_i$ and V_m in the development of cardiac alternans

The multitude of experimental conditions and interventions that cause and modulate Ca^{2+} and electromechanical alternans have undoubtedly demonstrated that cardiac alternans is a multifactorial process. While it is well accepted that electrical (APD), mechanical and CaT alternans strongly correlate [23, 53, 54], a comprehensive mechanism that can explain and predict the occurrence of cardiac alternans has not been fully established to date, although recently progress was made towards a unifying overarching conceptual framework for alternans in ventricular myocytes[14, 55–57]. In addition, in the process of a unifying theory of cardiac alternans invaluable insight has come from computational models of cardiac Ca^{2+} signaling and ion current activity during ECC and APD alternans (for comprehensive reviews and references see[9, 10, 14]). The key concept behind these computational models is the paradigm that the beat-to-beat regulation of V_m and $[Ca^{2+}]_i$ are bi-directionally coupled, and feedback mechanisms, often mediated by Ca^{2+}, play a crucial role. Bi-directional coupling of V_m and $[Ca^{2+}]_i$ is defined by the facts that 1) V_m directly determines the activity of Ca^{2+} handling mechanisms that are voltage-dependent ($V_m \rightarrow [Ca^{2+}]_i$ coupling), whereas 2) $[Ca^{2+}]_i \rightarrow V_m$ coupling is determined by the effect of Ca^{2+}-dependent ion currents and transporters. In current clamp experiments (Fig. 1) we confirmed that Ca^{2+} and APD alternans were closely coupled in both atrial and ventricular myocytes. Alternans developed at pacing rates >1 Hz (Suppl. Fig. I), there was no temporal dispersion in the onset of CaT and APD alternans, and the degree of APD and CaT alternans correlated closely (Fig. 2). Furthermore, we investigated which direction of coupling - $V_m \rightarrow [Ca^{2+}]_i$ or $[Ca^{2+}]_i \rightarrow V_m$ - plays the key role in the development of cardiac alternans.

$V_m \rightarrow [Ca^{2+}]_i$ coupling and cardiac alternans—Previous studies have suggested a primary role of $[Ca^{2+}]_i \rightarrow V_m$ in ventricular cells [22, 27, 29, 58], however for atrial myocytes the data are scarce. Thus, we aimed to collect direct experimental evidence in favor of or against $V_m \rightarrow [Ca^{2+}]_i$ coupling in atrial cells and compare with data obtained from ventricular myocytes. We designed an experimental approach where V_m was treated as an independent variable and $[Ca^{2+}]_i$ was viewed as the dependent parameter controlled by V_m. Application of series of same-shape AP waveforms (AP_{CaT_Large} (Fig. 3 A,C) or AP_{CaT_Small} (Fig. 3 B, D)) resulted in CaT alternans in both atrial and ventricular myocytes, i.e. CaT alternans developed, provided the pacing rate was sufficiently high, irrespective of AP duration and shape. In a next set of experiments we applied a voltage clamp protocol that consisted of APs with alternating duration, termed ‘alternans AP clamp’. As shown in Fig. 4 with the ‘alternans AP clamp’ protocol three qualitatively different Ca^{2+} responses could be elicited: 1) no CaT alternans; 2) “in-phase” alternans where the large CaT was observed with the AP_{CaT_Large} command, and 3) “out-of-phase” alternans where the large Ca^{2+} signal coincided with AP_{CaT_Small}. Thus, the AP voltage clamp experiments clearly demonstrate that CaT alternans can develop in the absence or presence of APD alternans. Furthermore, the identical ‘alternans AP clamp’ protocol could elicit “in-phase” and “out-of-phase” alternans in the same individual cell, arguing against the possibility that these results could be attributed to variability between cells. These results strongly argue against $V_m \rightarrow [Ca^{2+}]_i$ coupling being a dominant causative factor for the generation of CaT alternans in both atrial and ventricular myocytes.

$[Ca^{2+}]_i \rightarrow V_m$ coupling and cardiac alternans—Additional support for the paradigm that $[Ca^{2+}]_i \rightarrow V_m$ coupling as the primary cause of atrial alternans was obtained from the experiments shown in Fig. 6. In current clamp experiments combined with simultaneous $[Ca^{2+}]_i$ measurements atrial myocytes that revealed stable APD and CaT alternans were exposed to ryanodine to eliminate SR Ca^{2+} release without affecting Ca^{2+} entry via I_{LCC}. Ryanodine treatment completely abolished SR Ca^{2+} release and subsequently CaT alternans, and at the same time stabilized APD and AP morphology. The observation of elimination of alternans by ryanodine in atrial myocytes is consistent with earlier finding obtained mainly (but see also[59]) in ventricular tissue[22, 51, 52]. In addition, we have shown previously that beat-to-beat restitution properties of SR Ca^{2+} release[28], as well as the interplay between mitochondria[60, 61], cellular metabolism[54, 62] and Ca^{2+} signaling influence the likelihood of cardiac alternans, providing altogether strong evidence that the primary cause of cardiac alternans lies in disturbances of cellular beat-to-beat Ca^{2+} signaling.

Putative mechanisms of CaT alternans

While evidence in favor of $[Ca^{2+}]_i \rightarrow V_m$ coupling as the primary cause of alternans is growing, it is still unresolved which disturbances of Ca^{2+} regulatory mechanisms and processes are ultimately responsible for CaT alternans. Here we summarize, in the context of our new experimental data, putative mechanisms.

SR Ca^{2+} load and CaT alternans—Under steady-state conditions SR Ca^{2+} release and uptake by SERCA are well balanced, resulting in little beat-to-beat variation in diastolic $[Ca^{2+}]_{SR}$. If the balance between Ca^{2+} uptake and release is disturbed beat-to-beat alternation in diastolic $[Ca^{2+}]_{SR}$ might occur. Since oscillations in diastolic SR Ca^{2+} load have been observed [27, 50] it didn't come as a surprise that beat-to-beat instabilities in $[Ca^{2+}]_{SR}$ were proposed as an underlying mechanism of alternans [27, 63]. Due to the steep SR load – Ca^{2+} release relationship a higher SR load is expected to lead to a larger CaT and *vice versa*. However, contrary to these observations, others have reported CaT alternans without significant change in end-diastolic SR load in single myocytes [28, 54, 64] and intact heart [65] indicating that alternation in diastolic $[Ca^{2+}]_{SR}$ is not a required condition for CaT alternans to occur. Particularly in atrial myocytes the absence of diastolic $[Ca^{2+}]_{SR}$ alternans during cytosolic alternans was a common observation [28, 54, 58] and might be related to the lower expression of the endogenous SERCA inhibitor phospholamban [36–38] and a higher activity of SERCA and capacity to completely refill the SR on every beat.

I_{LCC} and CaT alternans—Under the concept of bi-directional coupling of $[Ca^{2+}]_i$ and V_m, I_{LCC} plays a unique role: I_{LCC} represents the critical trigger for CICR, and SR Ca^{2+} release (and ultimately the amount of Ca^{2+} that becomes available for contraction) is graded with I_{LCC}. The activity of I_{LCC} is controlled by voltage and Ca^{2+} itself: activation of I_{LCC} is voltage-dependent, and inactivation of the currents is subject to a complex voltage- and Ca^{2+}-dependence. Thus, it comes as no surprise that beat-to-beat alternations of I_{LCC} have been proposed as a causative factor of CaT alternans. A potential mechanism would entail incomplete time-dependent recovery from inactivation of I_{LCC}[48–50], and a reduced I_{LCC} was indeed shown to increase susceptibility to CaT alternans[27]. This hypothesis, however would

have to reconcile the observation that peak I_{LCC} is unchanged during alternans in both ventricular and atrial myocytes (Fig. 5B, see also [27–30, 54]).

Under the premise that during CaT alternans a large-amplitude CaT requires a larger I_{LCC} one would expect a larger I_{LCC} also to lead to a more pronounced plateau phase and a prolongation of APD. However we observed the opposite: APD30, which is recorded at V_m levels that are near maximal activation of I_{LCC}, was shorter during the large amplitude CaT and prolonged when intracellular Ca^{2+} release was small. These results, however can be - at least in part - explained by the observation that the large CaT enhances CDI of I_{LCC} (Fig. 5A) and thus the channel inactivates more rapidly and hence shortens the AP. CDI observed in the cells stimulated with square voltage pulses (Fig. 5) was relatively small, and hardly can account alone for a substantially shorter APD accompanying the large CaT. Consequently, this indicates that other Ca^{2+}-dependent conductances (such as Na/Ca exchange (NCX), non-selective cation [66], Ca^{2+}-activated Cl^- [67], small conductance Ca^{2+}-activated K^+ current[50]) also might play a role in the generation of APD alternans. These experimental findings clearly illustrate that disturbances in $[Ca^{2+}]_i \rightarrow V_m$ coupling profoundly affect the electrical stability of the cell, and how intricate and complex feedback mechanisms involving Ca^{2+}-dependent membrane conductances mediate AP instabilities.

Refractoriness of ryanodine receptors and CaT alternans—Finally, refractoriness of the SR Ca^{2+} release machinery was suggested as a possible mechanism responsible for CaT alternans [28, 65]. This idea was also supported by *in-silico* simulations[39]. In this case, it is hypothesized that the sum of ryanodine receptors (RyRs) (possibly in conjunction with other elements of the SR Ca^{2+} release mechanism) show different beat-to-beat degrees and kinetics of recovery from inactivation. The number of available release channels at any given beat depend on how many channels have recovered from previous release. Since the amplitude of a CaT is dictated by the number of activated RyRs, a large CaT will leave a larger fraction of RyRs in an inactivated state and therefore potentially unavailable for subsequent release and, provided the diastolic interval is short enough, leading to a smaller CaT. We have shown previously that in rabbit atrial myocytes RyR refractoriness is indeed prolonged after a large amplitude CaT and the kinetics of RyR recovery from inactivation is a key factor in the generation of CaT alternans[28].

Alternans in atrial and ventricular myocytes

The main aim of this study was to establish whether $V_m \rightarrow [Ca]_i$ or $[Ca]_i \rightarrow V_m$ coupling is the primary mechanism for alternans in atrial cells. To date, this question has been addressed primarily in ventricular tissue[10, 14, 22] and to a much lesser extent in atrial myocytes. To allow for reliable comparison between mechanisms of alternans in atrium and ventricle, we performed analogous experiments under the same conditions in both types of cardiomyocytes. While it is anticipated that mechanisms of alternans in atrial and ventricular cells will share similarities, significant differences are also expected. The main structural difference between ventricular and atrial myocytes is that atrial cells lack or have only a poorly or irregularly developed t-tubule system,[33–35] resulting in unique Ca^{2+} cycling features during ECC. In atrial myocytes lacking t-tubules LCCs are located only in the periphery of the cell and thus, membrane depolarization induced Ca^{2+} release first occurs in

subsarcolemmal regions and then propagates to the center of the cell. Computer simulations using cell models with and without t-tubules have predicted significant differences in possible alternans mechanisms[39–41]. The cardiac cell models lacking t-tubules exhibited higher likelihood to develop CaT alternans and pointed towards the role of Ca^{2+} diffusion, inhomogeneities in $[Ca]_i$[41] and RyR refractoriness[39] in the process. This is consistent with spatial and temporal inhomogeneities in $[Ca^{2+}]_i$ during atrial alternans found experimentally. As we have shown previously[54, 58, 62] during alternans especially the small amplitude CaT was spatially inhomogeneous, there are intracellular gradients of the AR and subcellular regions can alternate out-of-phase. The latter is of particular interest since the border between subcellular regions alternating out-of-phase is highly susceptible to spontaneous arrhythmogenic Ca^{2+} release and represent a frequent site of origin of spontaneous Ca^{2+} waves. Another difference in Ca^{2+} handling between atrial and ventricular cells is the lower expression of phospholamban that leads to higher SERCA activity in the atria [36–38]. The beat-to-beat fluctuation in SR load was proposed as a possible cause of CaT alternans [27, 63]. It is conceivable that the lower SERCA activity in ventricle may contribute to CaT alternans at increased pacing frequencies due to incomplete filling of the SR, whereas a more rapid filling is consistent with the observation that in atrial cells end-diastolic $[Ca^{2+}]_{SR}$ typically did not alternate during CaT alternans [28, 58].

In this study, irrespective of whether current clamp experiments were conducted in atrial or ventricular myocytes, CaT and APD alternans coincided closely and the degree of CaT and APD alternans correlated well (Figures 1 and 2). In both cell types the biggest beat-to-beat difference in APD was observed at APD30 (corresponding essentially to the plateau phase of the AP). Nonetheless, there were subtle differences between atrial and ventricular myocytes and measured relative beat-to-beat differences in APD were larger in atrial myocytes. In addition, a slightly higher pacing frequency was needed to induce alternans in atrial myocytes (Suppl. Fig. I). The basis of this difference between atrial and ventricular cells remains unclear. It is likely that degree of APD alternans is determined by the distinctive set of ion channels and transporters typical for each cell type. For example, ventricle and atrium differ in the activity of Ca^{2+}-activated small conductance K^+ [68, 69] and Ca^{2+}-activated Cl^- channels[70], while acetylcholine-activated and ultrarapid rectifier K^+ channels are expressed exclusively in the atria[71–73]. On the other hand, duration of the atrial AP is significantly shorter and this per se can result in the bigger relative change of APD, even if atrial and ventricular cells share similar Ca^{2+}-dependent mechanisms leading to APD alternation.

To recreate V_m changes occurring during APD alternans, voltage clamped cardiomyocytes were paced with cell type specific ‘alternans AP clamp’ voltage protocols. These experiments demonstrated that CaT alternans can be “in-phase” or “out-of-phase” in both atrial and ventricular myocytes (Fig. 4E), i.e. a large amplitude CaT can coincide with AP_{CaT_Large} or with AP_{CaT_Small}. Most atrial cells showed exclusively “in-phase” alternans, and no atrial cell showed exclusively “out-of-phase” alternans. In contrast, the majority of ventricular cells revealed both, “in-phase” and “out-of-phase” alternans and there was a fraction of ventricular cells that showed exclusively “out-of-phase” alternans. This finding suggests that $V_m \rightarrow [Ca^{2+}]_i$ coupling might play a more prominent role in atrial than in ventricular cells. In contrast, there seems to be a higher degree of independence of CaT

alternans from AP morphology in ventricular cells. Atrial cells, however, have a bigger relative beat-to-beat difference in APD. It is expected that the alternating voltage will affect activity of LCC and Ca^{2+} removal by NCX, and thus will significantly modulate stability and severity of CaT alternans. In addition, the shape of the AP was shown to modulate SR Ca^{2+} load[74]. Therefore, the bigger relative alternation in APD might make atria more susceptible to alternans and arrhythmias.

Summary and conclusions

With the combined use of the patch clamp technique and intracellular Ca^{2+} indicator dyes we demonstrate that cardiac alternans arise from disturbances of intracellular Ca^{2+} signaling and that the concomitant characteristic changes in AP morphology are secondary to changes in $[Ca^{2+}]_i$ and mediated through mechanisms discussed in details. The causes of Ca^{2+} and electromechanical alternans are multiple and reflect the inherently complex beat-to-beat regulation of $[Ca^{2+}]_i$ and V_m, referred to here as the bi-directional coupling of $[Ca^{2+}]_i$ and V_m. It has become increasingly clear that cardiac alternans are predominantly driven by $[Ca^{2+}]_i \rightarrow V_m$ coupling, however through complex feedback mechanisms $V_m \rightarrow [Ca^{2+}]_i$ coupling plays a modulatory role in the regulation of alternans. In our study striking similarities between atrial and ventricular cells with respect to the importance of $[Ca^{2+}]_i \rightarrow V_m$ coupling were found. However, larger alternations of APD implies a potentially more prominent role of $V_m \rightarrow [Ca^{2+}]_i$ coupling in modulation of alternans in the atria.

Supplementary Material

Refer to Web version on PubMed Central for supplementary material.

Acknowledgments

SOURCES OF FUNDING

This work was supported by National Institutes of Health grants HL62231, HL80101 and HL101235 and the Leducq Foundation (to LAB).

Nonstandard Abbreviations and Acronyms

AP	action potential
AP_{CaT_Large}	AP recorded during a large amplitude alternans Ca^{2+} transient
AP_{CaT_Small}	AP recorded during a small amplitude alternans Ca^{2+} transient
APD	action potential duration
AR	alternans ratio
$[Ca^{2+}]_{SR}$	SR Ca^{2+} concentration
CaT	Ca^{2+} transient
CDI	Ca^{2+}-dependent inactivation
CICR	Ca^{2+}-induced Ca^{2+} release

ECC	excitation-contraction coupling
I_{LCC}	L-type Ca^{2+} channel current
I_{NCX}	Na/Ca exchange current
R	ratio of background subtracted Indo-1 fluorescence emission at 410 nm and 485 nm
RyR	ryanodine receptor
SERCA	sarcoplasmic/endoplasmic reticulum Ca^{2+} ATPase
SR	sarcoplasmic reticulum
V_m	membrane potential

References

1. Comtois P, Nattel S. Atrial repolarization alternans as a path to atrial fibrillation. J Cardiovasc Electrophysiol. 2012; 23:1013–1015. [PubMed: 22788865]
2. Hiromoto K, Shimizu H, Furukawa Y, Kanemori T, Mine T, Masuyama T, Ohyanagi M. Discordant repolarization alternans-induced atrial fibrillation is suppressed by verapamil. Circ J. 2005; 69:1368–1373. [PubMed: 16247213]
3. Narayan SM, Franz MR, Clopton P, Pruvot EJ, Krummen DE. Repolarization alternans reveals vulnerability to human atrial fibrillation. Circulation. 2011; 123:2922–2930. [PubMed: 21646498]
4. Walker ML, Rosenbaum DS. Repolarization alternans: Implications for the mechanism and prevention of sudden cardiac death. Cardiovascular research. 2003; 57:599–614. [PubMed: 12618222]
5. Ter Keurs HE, Boyden PA. Calcium and arrhythmogenesis. Physiological reviews. 2007; 87:457–506. [PubMed: 17429038]
6. Verrier RL, Nieminen T. T-wave alternans as a therapeutic marker for antiarrhythmic agents. J Cardiovasc Pharmacol. 2010; 55:544–554. [PubMed: 20555232]
7. Verrier RL, Klingenheben T, Malik M, El-Sherif N, Exner DV, Hohnloser SH, Ikeda T, Martinez JP, Narayan SM, Nieminen T, Rosenbaum DS. Microvolt T-wave alternans testing has a role in arrhythmia risk stratification. J Am Coll Cardiol. 2012; 59:1572–1573. [PubMed: 22516453]
8. Wohlfart B. Analysis of mechanical alternans in rabbit papillary muscle. Acta Physiologica Scandinavica. 1982; 115:405–414. [PubMed: 6184949]
9. Weiss JN, Karma A, Shiferaw Y, Chen PS, Garfinkel A, Qu Z. From pulsus to pulseless: The saga of cardiac alternans. Circulation research. 2006; 98:1244–1253. [PubMed: 16728670]
10. Weiss JN, Nivala M, Garfinkel A, Qu Z. Alternans and arrhythmias: From cell to heart. Circulation research. 2011; 108:98–112. [PubMed: 21212392]
11. Clusin WT. Mechanisms of calcium transient and action potential alternans in cardiac cells and tissues. Am J Physiol Heart Circ Physiol. 2008; 294:H1–H10. [PubMed: 17951365]
12. Merchant FM, Armoundas AA. Role of substrate and triggers in the genesis of cardiac alternans, from the myocyte to the whole heart: Implications for therapy. Circulation. 2012; 125:539–549. [PubMed: 22271847]
13. Gaeta SA, Christini DJ. Non-linear dynamics of cardiac alternans: Subcellular to tissue-level mechanisms of arrhythmia. Front Physiol. 2012; 3:157. [PubMed: 22783195]
14. Qu Z, Nivala M, Weiss JN. Calcium alternans in cardiac myocytes: Order from disorder. J Mol Cell Cardiol. 2013; 58:100–109. [PubMed: 23104004]
15. Mahajan A, Shiferaw Y, Sato D, Baher A, Olcese R, Xie LH, Yang MJ, Chen PS, Restrepo JG, Karma A, Garfinkel A, Qu Z, Weiss JN. A rabbit ventricular action potential model replicating cardiac dynamics at rapid heart rates. Biophys J. 2008; 94:392–410. [PubMed: 18160660]

16. Nolasco JB, Dahlen RW. A graphic method for the study of alternation in cardiac action potentials. J Appl Physiol. 1968; 25:191–196. [PubMed: 5666097]
17. Tolkacheva EG, Anumonwo JM, Jalife J. Action potential duration restitution portraits of mammalian ventricular myocytes: Role of calcium current. Biophys J. 2006; 91:2735–2745. [PubMed: 16844743]
18. Tolkacheva EG, Romeo MM, Guerraty M, Gauthier DJ. Condition for alternans and its control in a two-dimensional mapping model of paced cardiac dynamics. Phys Rev E Stat Nonlin Soft Matter Phys. 2004; 69:031904. [PubMed: 15089319]
19. Watanabe MA, Koller ML. Mathematical analysis of dynamics of cardiac memory and accommodation: Theory and experiment. Am J Physiol Heart Circ Physiol. 2002; 282:H1534–1547. [PubMed: 11893591]
20. Koller ML, Maier SK, Gelzer AR, Bauer WR, Meesmann M, Gilmour RF Jr. Altered dynamics of action potential restitution and alternans in humans with structural heart disease. Circulation. 2005; 112:1542–1548. [PubMed: 16157783]
21. Gelzer AR, Koller ML, Otani NF, Fox JJ, Enyeart MW, Hooker GJ, Riccio ML, Bartoli CR, Gilmour RF Jr. Dynamic mechanism for initiation of ventricular fibrillation in vivo. Circulation. 2008; 118:1123–1129. [PubMed: 18725487]
22. Goldhaber JI, Xie LH, Duong T, Motter C, Khuu K, Weiss JN. Action potential duration restitution and alternans in rabbit ventricular myocytes: The key role of intracellular calcium cycling. Circ Res. 2005; 96:459–466. [PubMed: 15662034]
23. Pruvot EJ, Katra RP, Rosenbaum DS, Laurita KR. Role of calcium cycling versus restitution in the mechanism of repolarization alternans. Circ Res. 2004; 94:1083–1090. [PubMed: 15016735]
24. Saitoh H, Bailey JC, Surawicz B. Alternans of action potential duration after abrupt shortening of cycle length: Differences between dog purkinje and ventricular muscle fibers. Circ Res. 1988; 62:1027–1040. [PubMed: 3359572]
25. Banville I, Gray RA. Effect of action potential duration and conduction velocity restitution and their spatial dispersion on alternans and the stability of arrhythmias. J Cardiovasc Electrophysiol. 2002; 13:1141–1149. [PubMed: 12475106]
26. Wu R, Patwardhan A. Mechanism of repolarization alternans has restitution of action potential duration dependent and independent components. J Cardiovasc Electrophysiol. 2006; 17:87–93. [PubMed: 16426408]
27. Diaz ME, O'Neill SC, Eisner DA. Sarcoplasmic reticulum calcium content fluctuation is the key to cardiac alternans. Circ Res. 2004; 94:650–656. [PubMed: 14752033]
28. Shkryl VM, Maxwell JT, Domeier TL, Blatter LA. Refractoriness of sarcoplasmic reticulum Ca release determines Ca alternans in atrial myocytes. Am J Physiol Heart Circ Physiol. 2012; 302:H2310–2320. [PubMed: 22467301]
29. Chudin E, Goldhaber J, Garfinkel A, Weiss J, Kogan B. Intracellular Ca(2+) dynamics and the stability of ventricular tachycardia. Biophys J. 1999; 77:2930–2941. [PubMed: 10585917]
30. Wan X, Laurita KR, Pruvot EJ, Rosenbaum DS. Molecular correlates of repolarization alternans in cardiac myocytes. J Mol Cell Cardiol. 2005; 39:419–428. [PubMed: 16026799]
31. Naccarelli GV, Varker H, Lin J, Schulman KL. Increasing prevalence of atrial fibrillation and flutter in the united states. Am J Cardiol. 2009; 104:1534–1539. [PubMed: 19932788]
32. Jousset F, Tenkorang J, Vesin JM, Pascale P, Ruchat P, Rollin AG, Fromer M, Narayan SM, Pruvot E. Kinetics of atrial repolarization alternans in a free-behaving ovine model. J Cardiovasc Electrophysiol. 2012; 23:1003–1012. [PubMed: 22554055]
33. Pawlak Cieslik A, Szturmowicz M, Fijalkowska A, Gatarek J, Gralec R, Blasinska-Przerwa K, Szczepulska-Wojcik E, Skoczylas A, Bilska A, Tomkowski W. Diagnosis of malignant pericarditis: A single centre experience. Kardiol Pol. 2012; 70:1147–1153. [PubMed: 23180523]
34. Bootman MD, Smyrnias I, Thul R, Coombes S, Roderick HL. Atrial cardiomyocyte calcium signalling. Biochim Biophys Acta. 2011; 1813:922–934. [PubMed: 21295621]
35. Sheehan KA, Zima AV, Blatter LA. Regional differences in spontaneous Ca^{2+} spark activity and regulation in cat atrial myocytes. J Physiol. 2006; 572:799–809. [PubMed: 16484302]
36. Boknik P, Unkel C, Kirchhefer U, Kleideiter U, Klein-Wiele O, Knapp J, Linck B, Luss H, Muller FU, Schmitz W, Vahlensieck U, Zimmermann N, Jones LR, Neumann J. Regional expression of

phospholamban in the human heart. Cardiovascular research. 1999; 43:67–76. [PubMed: 10536691]

37. Vangheluwe P, Schuermans M, Zador E, Waelkens E, Raeymaekers L, Wuytack F. Sarcolipin and phospholamban mRNA and protein expression in cardiac and skeletal muscle of different species. Biochem J. 2005; 389:151–159. [PubMed: 15801907]
38. Luss I, Boknik P, Jones LR, Kirchhefer U, Knapp J, Linck B, Luss H, Meissner A, Muller FU, Schmitz W, Vahlensieck U, Neumann J. Expression of cardiac calcium regulatory proteins in atrium vs ventricle in different species. J Mol Cell Cardiol. 1999; 31:1299–1314. [PubMed: 10371704]
39. Lugo CA, Cantalapiedra IR, Penaranda A, Hove-Madsen L, Echebarria B. Are SR Ca content fluctuations or SR refractoriness the key to atrial cardiac alternans?: Insights from a human atrial model. Am J Physiol Heart Circ Physiol. 2014; 306:H1540–1552. [PubMed: 24610921]
40. Tao T, O'Neill SC, Diaz ME, Li YT, Eisner DA, Zhang H. Alternans of cardiac calcium cycling in a cluster of ryanodine receptors: A simulation study. Am J Physiol Heart Circ Physiol. 2008; 295:H598–609. [PubMed: 18515647]
41. Li Q, O'Neill SC, Tao T, Li Y, Eisner D, Zhang H. Mechanisms by which cytoplasmic calcium wave propagation and alternans are generated in cardiac atrial myocytes lacking t-tubules-insights from a simulation study. Biophys J. 2012; 102:1471–1482. [PubMed: 22500747]
42. Heinzel FR, Bito V, Biesmans L, Wu M, Detre E, von Wegner F, Claus P, Dymarkowski S, Maes F, Bogaert J, Rademakers F, D'Hooge J, Sipido K. Remodeling of t-tubules and reduced synchrony of Ca^{2+} release in myocytes from chronically ischemic myocardium. Circ Res. 2008; 102:338–346. [PubMed: 18079411]
43. Lyon AR, MacLeod KT, Zhang Y, Garcia E, Kanda GK, Lab MJ, Korchev YE, Harding SE, Gorelik J. Loss of t-tubules and other changes to surface topography in ventricular myocytes from failing human and rat heart. Proc Natl Acad Sci U S A. 2009; 106:6854–6859. [PubMed: 19342485]
44. Balijepalli RC, Lokuta AJ, Maertz NA, Buck JM, Haworth RA, Valdivia HH, Kamp TJ. Depletion of t-tubules and specific subcellular changes in sarcolemmal proteins in tachycardia-induced heart failure. Cardiovascular research. 2003; 59:67–77. [PubMed: 12829177]
45. Wei S, Guo A, Chen B, Kutschke W, Xie YP, Zimmerman K, Weiss RM, Anderson ME, Cheng H, Song LS. T-tubule remodeling during transition from hypertrophy to heart failure. Circ Res. 2010; 107:520–531. [PubMed: 20576937]
46. Ordog B, Brutyo E, Puskas LG, Papp JG, Varro A, Szabad J, Boldogkoi Z. Gene expression profiling of human cardiac potassium and sodium channels. Int J Cardiol. 2006; 111:386–393. [PubMed: 16257073]
47. Wang Z, Yue L, White M, Pelletier G, Nattel S. Differential distribution of inward rectifier potassium channel transcripts in human atrium versus ventricle. Circulation. 1998; 98:2422–2428. [PubMed: 9832487]
48. Fox JJ, McHarg JL, Gilmour RF Jr. Ionic mechanism of electrical alternans. Am J Physiol Heart Circ Physiol. 2002; 282:H516–530. [PubMed: 11788399]
49. Shiferaw Y, Watanabe MA, Garfinkel A, Weiss JN, Karma A. Model of intracellular calcium cycling in ventricular myocytes. Biophys J. 2003; 85:3666–3686. [PubMed: 14645059]
50. Li Y, Diaz ME, Eisner DA, O'Neill S. The effects of membrane potential, SR Ca^{2+} content and RyR responsiveness on systolic Ca^{2+} alternans in rat ventricular myocytes. J Physiol. 2009; 587:1283–1292. [PubMed: 19153161]
51. Shimizu W, Antzelevitch C. Cellular and ionic basis for T-wave alternans under long-QT conditions. Circulation. 1999; 99:1499–1507. [PubMed: 10086976]
52. Saitoh H, Bailey JC, Surawicz B. Action potential duration alternans in dog purkinje and ventricular muscle fibers. Further evidence in support of two different mechanisms. Circulation. 1989; 80:1421–1431. [PubMed: 2553299]
53. Lee HC, Mohabir R, Smith N, Franz MR, Clusin WT. Effect of ischemia on calcium-dependent fluorescence transients in rabbit hearts containing Indo 1. Correlation with monophasic action potentials and contraction. Circulation. 1988; 78:1047–1059. [PubMed: 2844438]

54. Huser J, Wang YG, Sheehan KA, Cifuentes F, Lipsius SL, Blatter LA. Functional coupling between glycolysis and excitation-contraction coupling underlies alternans in cat heart cells. J Physiol. 2000; 524(Pt 3):795–806. [PubMed: 10790159]
55. Cui X, Rovetti RJ, Yang L, Garfinkel A, Weiss JN, Qu Z. Period-doubling bifurcation in an array of coupled stochastically excitable elements subjected to global periodic forcing. Phys Rev Lett. 2009; 103:044102. [PubMed: 19659359]
56. Rovetti R, Cui X, Garfinkel A, Weiss JN, Qu Z. Spark-induced sparks as a mechanism of intracellular calcium alternans in cardiac myocytes. Circ Res. 2010; 106:1582–1591. [PubMed: 20378857]
57. Nivala M, Qu Z. Calcium alternans in a couplon network model of ventricular myocytes: Role of sarcoplasmic reticulum load. Am J Physiol Heart Circ Physio l. 2012; 303:H341–352.
58. Edwards JN, Blatter LA. Cardiac alternans and intracellular calcium cycling. Clin Exp Pharmacol Physiol. 2014; 41:524–532. [PubMed: 25040398]
59. Llach A, Molina CE, Fernandes J, Padro J, Cinca J, Hove-Madsen L. Sarcoplasmic reticulum and L-type Ca^{2+} channel activity regulate the beat-to-beat stability of calcium handling in human atrial myocytes. J Physiol. 2011; 589:3247–3262. [PubMed: 21521767]
60. Florea SM, Blatter LA. The role of mitochondria for the regulation of cardiac alternans. Front Physio. 2010; 1:1–9.
61. Florea SM, Blatter LA. Regulation of cardiac alternans by beta-adrenergic signaling pathways. Am J Physiol Heart Circ Physiol. 2012; 303:H1047–1056. [PubMed: 22904161]
62. Kockskamper J, Blatter LA. Subcellular Ca^{2+} alternans represents a novel mechanism for the generation of arrhythmogenic Ca^{2+} waves in cat atrial myocytes. J Physiol. 2002; 545:65–79. [PubMed: 12433950]
63. Eisner DA, Li Y, O'Neill SC. Alternans of intracellular calcium: Mechanism and significance. Heart Rhythm. 2006; 3:743–745. [PubMed: 16731482]
64. Picht E, DeSantiago J, Blatter LA, Bers DM. Cardiac alternans do not rely on diastolic sarcoplasmic reticulum calcium content fluctuations. Circ Res. 2006; 99:740–748. [PubMed: 16946134]
65. Wang L, Myles RC, De Jesus NM, Ohlendorf AK, Bers DM, Ripplinger CM. Optical mapping of sarcoplasmic reticulum Ca^{2+} in the intact heart: Ryanodine receptor refractoriness during alternans and fibrillation. Circ Res. 2014; 114:1410–1421. [PubMed: 24568740]
66. Simard C, Hof T, Keddache Z, Launay P, Guinamard R. The TRPM4 non-selective cation channel contributes to the mammalian atrial action potential. J Mol Cell Cardiol. 2013; 59:11–19. [PubMed: 23416167]
67. Guo D, Young L, Patel C, Jiao Z, Wu Y, Liu T, Kowey PR, Yan GX. Calcium-activated chloride current contributes to action potential alternations in left ventricular hypertrophy rabbit. Am J Physiol Heart Circ Physiol. 2008; 295:H97–H104. [PubMed: 18441200]
68. Tuteja D, Xu D, Timofeyev V, Lu L, Sharma D, Zhang Z, Xu Y, Nie L, Vazquez AE, Young JN, Glatter KA, Chiamvimonvat N. Differential expression of small-conductance Ca^{2+}-activated K^+ channels SK1, SK2, and SK3 in mouse atrial and ventricular myocytes. Am J Physiol Heart Circ Physiol. 2005; 289:H2714–2723. [PubMed: 16055520]
69. Hsueh CH, Chang PC, Hsieh YC, Reher T, Chen PS, Lin SF. Proarrhythmic effect of blocking the small conductance calcium activated potassium channel in isolated canine left atrium. Heart Rhythm. 2013; 10:891–898. [PubMed: 23376397]
70. Szigeti G, Rusznak Z, Kovacs L, Papp Z. Calcium-activated transient membrane currents are carried mainly by chloride ions in isolated atrial, ventricular and purkinje cells of rabbit heart. Exp Physiol. 1998; 83:137–153. [PubMed: 9568474]
71. Dobrzynski H, Marples DD, Musa H, Yamanushi TT, Henderson Z, Takagishi Y, Honjo H, Kodama I, Boyett MR. Distribution of the muscarinic K^+ channel proteins kir3.1 and kir3.4 in the ventricle, atrium, and sinoatrial node of heart. J Histochem Cytochem. 2001; 49:1221–1234. [PubMed: 11561006]
72. Bingen BO, Neshati Z, Askar SF, Kazbanov IV, Ypey DL, Panfilov AV, Schalij MJ, de Vries AA, Pijnappels DA. Atrium-specific Kir3.X determines inducibility, dynamics, and termination of

fibrillation by regulating restitution-driven alternans. Circulation. 2013; 128:2732–2744. [PubMed: 24065610]

73. Ravens U, Wettwer E. Ultra-rapid delayed rectifier channels: Molecular basis and therapeutic implications. Cardiovasc Res. 2011; 89:776–785. [PubMed: 21159668]
74. Bassani RA, Altamirano J, Puglisi JL, Bers DM. Action potential duration determines sarcoplasmic reticulum Ca^{2+} reloading in mammalian ventricular myocytes. J Physiol. 2004; 559:593–609. [PubMed: 15243136]

Novelty and Significance

What Is Known?

- Cardiac alternans, described as beat-to-beat variation in contraction, action potential (AP) morphology and intracellular Ca^{2+} release, is a recognized risk factor for life-threatening arrhythmias.
- The interplay between intracellular Ca^{2+} handling, membrane potential and AP morphology underlies electromechanical alternans, however a mechanistic understanding of the alternans phenomenon is still incomplete.
- Previous studies investigating mechanisms of Ca^{2+} alternans have been performed mostly in ventricular but not in atrial tissue.

What New Information Does This Article Contribute?

- Beat-to-beat changes in AP duration (APD) and morphology alone are not sufficient to induce Ca^{2+} transients (CaT) alternans in atrial and ventricular myocytes.
- AP morphology alternans arise from disturbances of intracellular Ca^{2+} signaling.
- The underlying mechanisms of alternans reveal similarities in atrial and ventricular myocytes, however beat-to-beat changes in APD and voltage-dependent modulation of CaT alternans are more pronounced in the atrium.

Cardiac alternans is causatively linked to ventricular arrhythmias, atrial fibrillation, and sudden cardiac death. The mechanisms of alternans are complex and the bi-directional coupling between beat-to-beat cytosolic Ca^{2+} handling and membrane potential regulation is a key causative factor. This study, for the first time, investigated the relationship between AP morphology and CaT alternans in atria and compared the results with findings from ventricular tissue. In voltage-clamp experiments we showed that CaT alternans can be induced irrespective of the presence or absence of APD alternans, however suppression of Ca^{2+} release from sarcoplasmic reticulum abolished APD alternans. Our work reveals new insights into mechanisms and regulation of alternans in atrial cells and demonstrates that atrial and ventricular myocytes share many similarities in the underlying mechanisms, but also exhibit some important differences. Nonetheless, common to both tissues is the key finding that the occurrence of electromechanical alternans depends on beat-to-beat alternation of AP duration and morphology secondary to disturbances in Ca^{2+} signaling.

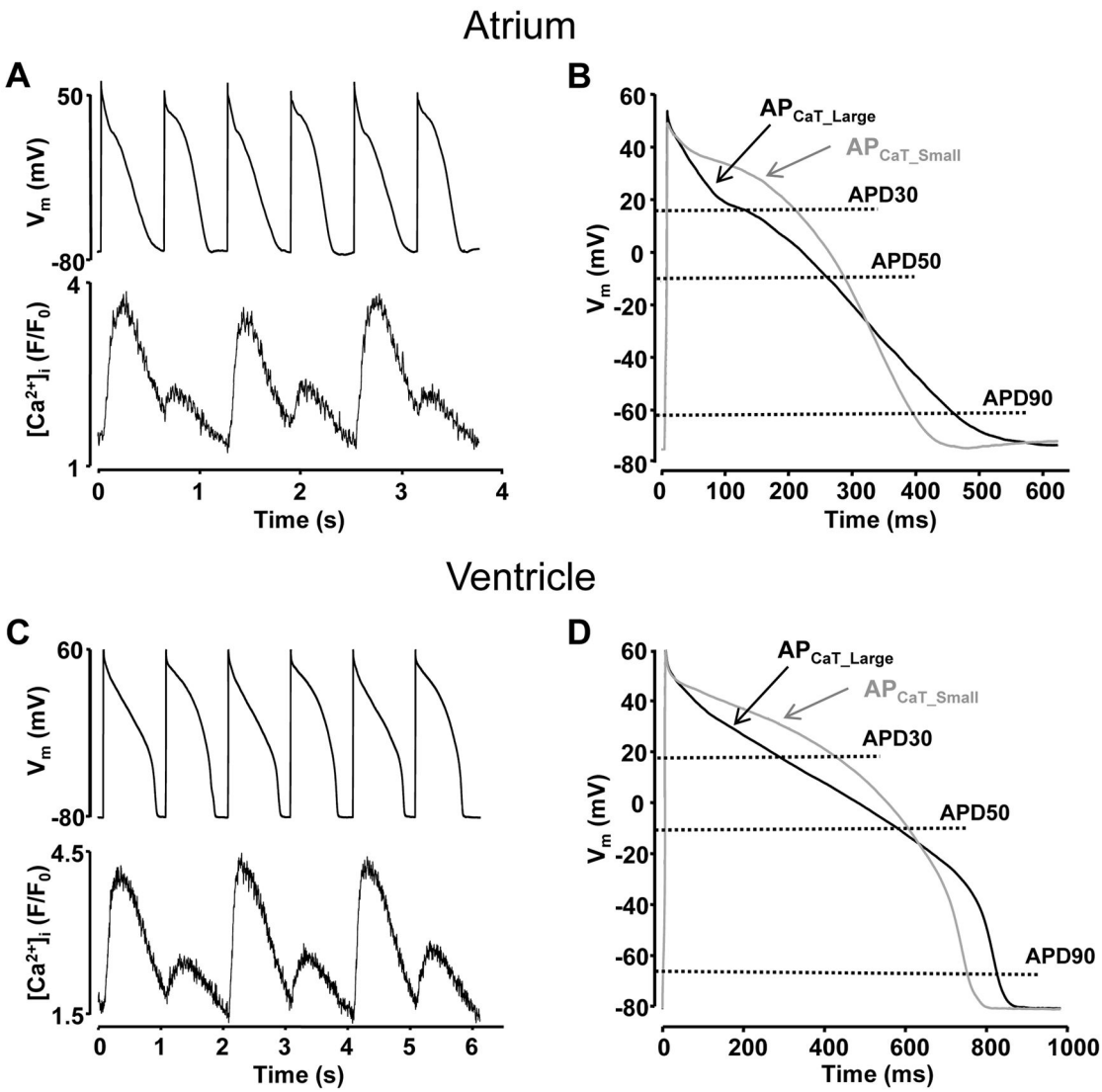

Figure 1. Simultaneous recordings of APD and CaT alternans in cardiac myocytes

A, C: Simultaneously recorded APs and CaTs in current-clamped atrial (**A**) and ventricular (**C**) myocytes. **B, D:** Superimposed AP traces recorded during large (black, AP_{CaT_Large}) and small (grey, AP_{CaT_Small}) amplitude CaTs from atrial (**B**) and ventricular (**D**) myocytes. AP waveforms are derived as an average of three consecutive AP_{CaT_Large} or AP_{CaT_Small} recordings.

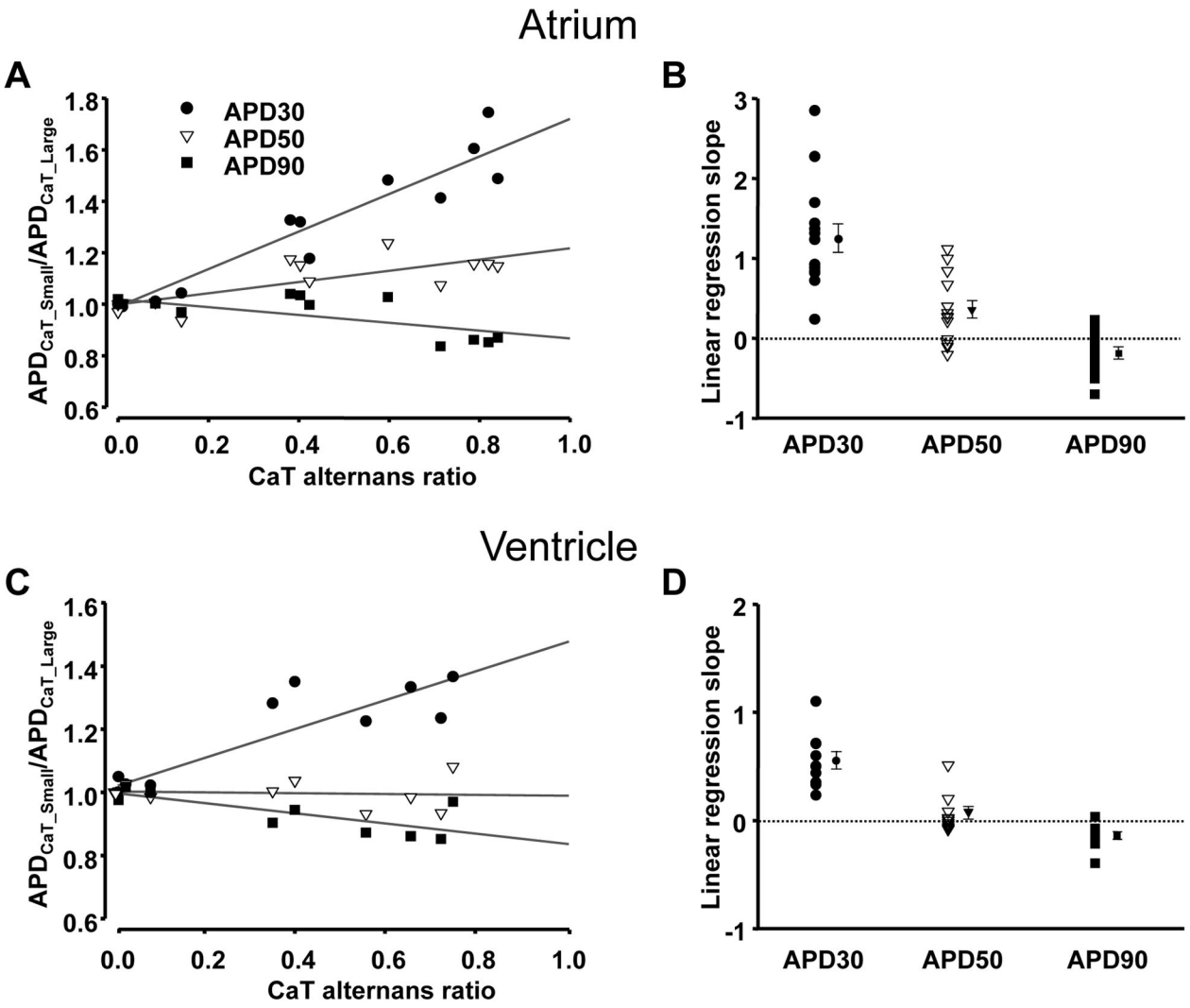

Figure 2. Correlation between APD and CaT alternans

A, C: Ratios of $APD30_{CaT\_Small}/APD30_{CaT\_Large}$ (●), $APD50_{CaT\_Small}/APD50_{CaT\_Large}$ (▽) and $APD90_{CaT\_Small}/APD90_{CaT\_Large}$ (■) plotted *versus* CaT alternans ratio recorded from the same atrial (**A**) and ventricular (**C**) myocyte as shown in Fig. 1. **B, D:** Range and mean ± SEM of linear regression slopes for APD30 (●), APD50 (▽) and APD90 (■) from atrial (**B**; n=14) and ventricular (**D**; n=10) myocytes.

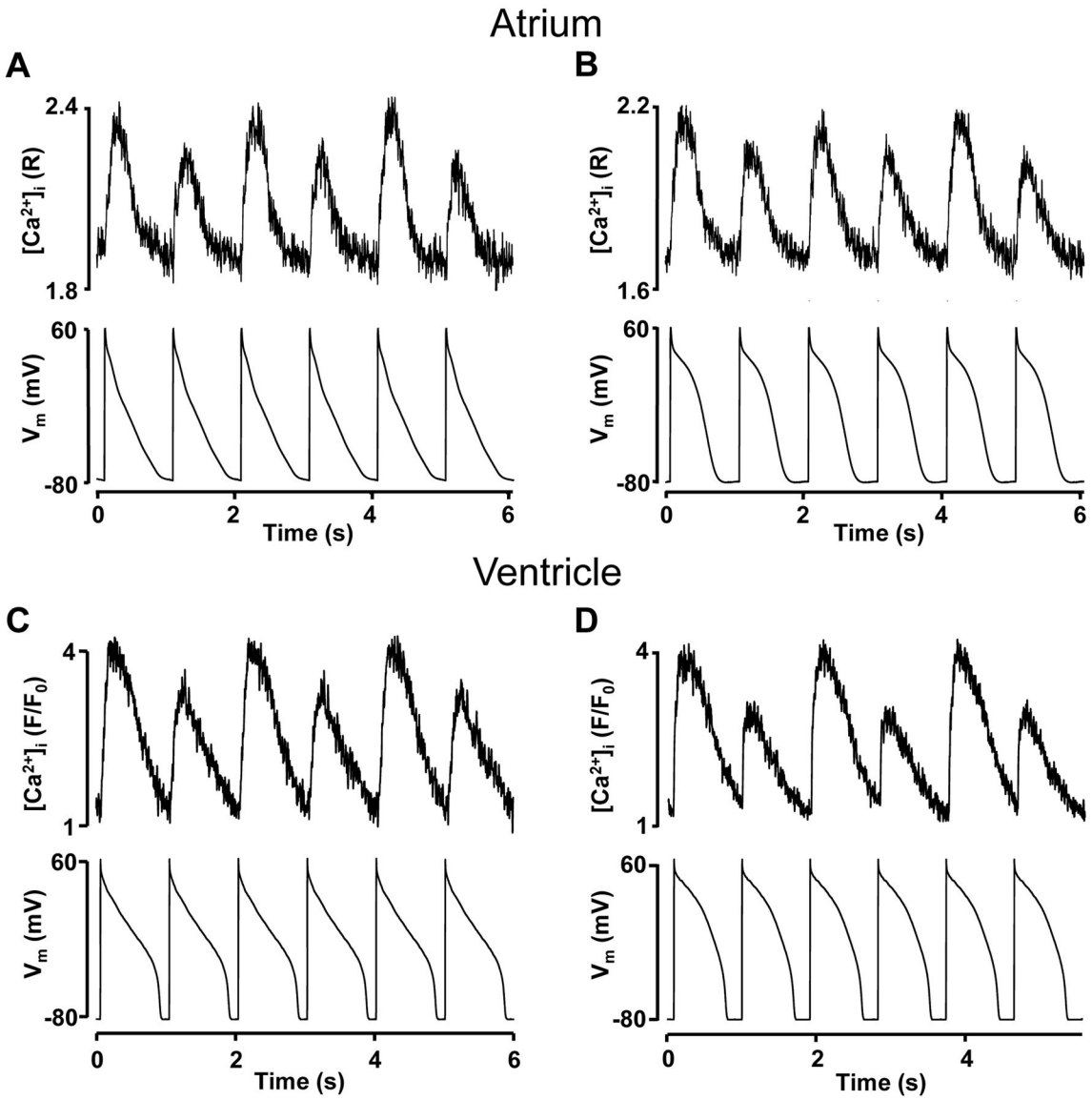

Figure 3. CaT alternans in voltage-clamped myocytes under constant AP-clamp conditions

A, B: CaT alternans recorded in voltage-clamped atrial myocytes paced with atrial same-shape AP_{CaT_Large}-AP_{CaT_Large} (**A**) or AP_{CaT_Small}-AP_{CaT_Small} (**B**) voltage clamp protocol (bottom trace). **C**, **D:** CaT alternans recorded in ventricular cells paced with ventricular same-shape AP_{CaT_Large}-AP_{CaT_Large} (**C**) and AP_{CaT_Small}-AP_{CaT_Small} (**D**) voltage protocols.

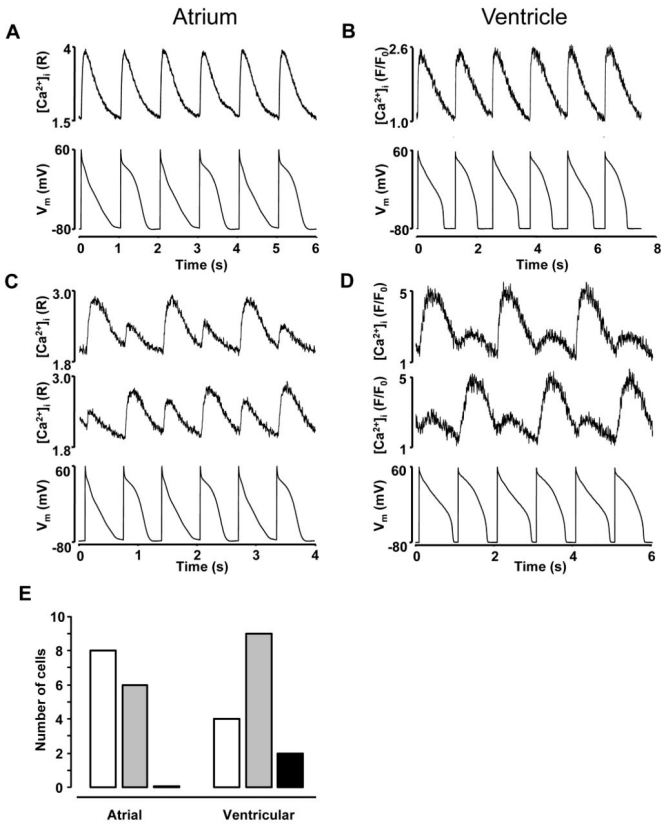

Figure 4. CaT alternans induced independently of cell voltage

A, B: At lower pacing frequencies CaT alternans was not observed in atrial (**A**) and ventricular (**B**) cells paced with the AP_{CaT_Large}-AP_{CaT_Small} voltage protocol referred to as 'alternans AP-clamp' (bottom trace). **C, D**: During 'alternans AP-clamp' large CaTs were observed with AP_{CaT_Large} ("in-phase", top trace) or with AP_{CaT_Small} ("out-of-phase", middle trace) voltage command (bottom). $[Ca^{2+}]_i$ traces were recorded from the same atrial (**C**) and ventricular (**D**) myocyte. **E:** Total number of atrial and ventricular myocytes exhibiting CaT alternans that were exclusively "in-phase" (▭), exclusively "out-of-phase" (■), or revealed both "in-phase" and "out-of-phase" alternans (▭).

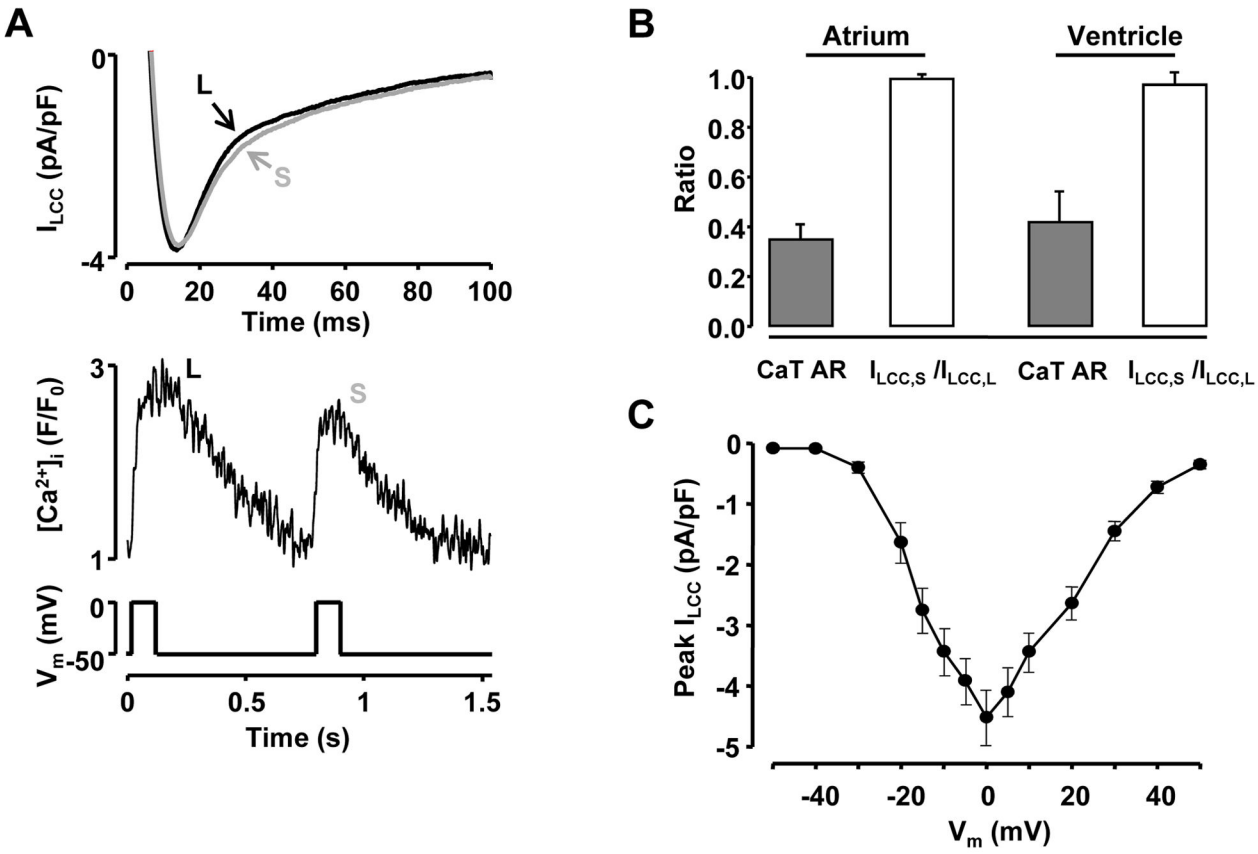

Figure 5. Simultaneous recordings of L-type Ca^{2+} current and CaT alternans

A: Simultaneous recordings of I_{LCC} and CaTs from a voltage-clamped ventricular myocyte during CaT alternans. I_{LCC} was elicited with 100 ms depolarization steps from a holding potential of -50 mV to 0 mV (bottom). S: small amplitude CaT; L: large amplitude CaT. **B:** Summary data for simultaneously recorded $I_{LCC,S}/I_{LCC,L}$ ratios and CaT AR in atrial (n=4) and ventricular (n=5) myocytes. $I_{LCC,S}$: peak L-type Ca^{2+} current recorded with small amplitude Ca^{2+} transient; $I_{LCC,L}$: peak current recorded simultaneously with large CaT. **C:** Current-voltage relationship of I_{LCC} recorded from ventricular myocytes (n=9).

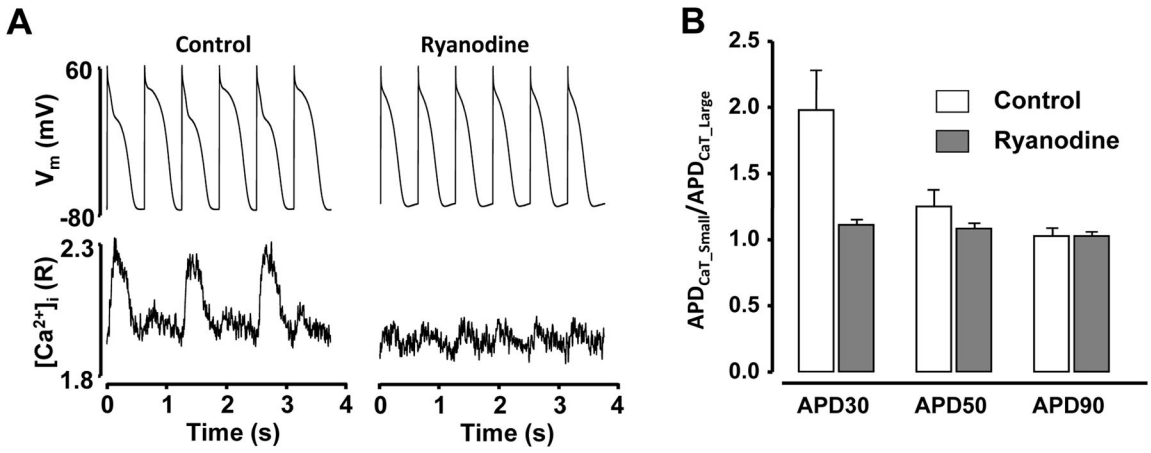

Figure 6. Inhibition of cytosolic Ca^{2+} release abolishes APD alternans

A: Application of 10 μmol/L ryanodine suppressed SR Ca^{2+} release and abolished APD and CaT alternans. AP and $[Ca^{2+}]_i$ were recorded simultaneously from a current-clamped atrial myocyte. **B:** Summary data for APD30CaT_Small/APD30CaT_Large, APD50CaT_Small/APD50CaT_Large and APD90CaT_Small/APD90CaT_Large ratios of atrial myocytes before (control) and after application of ryanodine (n=4).